Civil Engineering

Effect of floating bridges on bottom topography

Adnan D. Ghanim [a,*], M.M. Ibrahim [b], Mohamed A. Hassan [b]

[a] Advisor to the President of the Iraqi Council of Representatives, Iraq
[b] Shoubra Faculty of Engineering, Benha University, PO Box 11629, Shoubra, Egypt

ABSTRACT

Floating bridges are the practical answers for intersection enormous waterways with unordinary depth and exceptionally soft bottom where conventional piers are impractical. This paper describes experimentally the stability of bed material underneath the floating bridges under different hydraulic conditions introduced regarding flow discharge, tailgate water depth, the bridge length and the bridge draft for different loads over the bridge. Two distinctive bed materials are utilized to characterize the bed morphological changes. One hundred and sixty-eight tests are completed and the results are differentiated to the basic case where no bridges are introduced. The outcomes reveal that the particles size of bed material and the bridge draft are the dominant parameters that influence the bed morphology and flow attributes.
© 2020 The Authors. Published by Elsevier B.V. on behalf of Faculty of Engineering, Ain Shams University. This is an open access article under the CC BY license (http://creativecommons.org/licenses/by/4.0/).

1. Introduction

Bridges are normally successful methods for interfacing islands and landmasses with one another or potentially the territory. Without bridges, the development of roadways and railways crosswise over valleys and waterways would not be conceivable [1]. However, in certain occasions, a customary suspension or column bridge probably won't be achievable because of wide or deep water, or because the bed material is too soft to even consider supporting a pillar bridge foundation. For a site where the water is 2–5 km wide, 30–60 m deep and there is an exceptionally soft bottom stretching out another 30–60 m, a floating bridge is assessed to cost three to five times less than a long-length fixed bridge, tube, or tunnel [2].

Floating bridges have been utilized since ancient times around 4000 years ago. The principal sort of floating bridges are vessel spans, which are utilized in numerous fights [3]. The significance of this kind of bridges have turned out to be obvious in Europe during the Second World War (1939–1945) when the withdrawing

troops exploded the bridges built on waterways. The floating bridge are significant in the military activities [4]. Moreover, the floating bridges have been utilized as perpetual bridges in spots where the depth of water is excessively high, which anticipates the development of bridges on account of their heavy expenses [5].

The idea of a floating bridge exploits the natural law of buoyancy of water to support the dead and live loads. There is no requirement for conventional piers or foundations. However, an anchoring or structural system is expected to keep up transverse and longitudinal arrangements of the bridge. A modern floating bridge might be built of wood, concrete, steel, or a combination of materials, depending upon the structure prerequisites. A floating bridge is essentially a beam on a versatile foundation and supports which are characterized as pontoon-structures or semi-submersible structures [6]. A pontoon-structure is a floating component with a little depth contrasted with its width, and is reasonable in zones with calm water, for example, inside a bay or close to the coastline. Semi-submersible structures comprise of segments with watertight balance compartments connected to pontoons, and because of the counterbalance compartment, they are fitting for enormous wavelengths and wave heights.

Concentrating on loads, the floating bridges are exposed to different ecological loads, for example, wind and wave; as well as current loads, [7]. Yanyan [8] classifies the loads following up on the floating bridges into primary and secondary loads. The primary loads are dead, live, impact loads notwithstanding earth and hydrostatic pressures. However, the secondary loads are the wind and current loads in addition, the impacts because of the

---

* Corresponding author.
   E-mail address: adnanalghanam2016@gmail.com (A.D. Ghanim).
Peer review under responsibility of Ain Shams University.

Nomenclature

B	Flume width [m]	y_t	Tailgate water depth [m]
d	Submerged depth of the bridge [m]	ρ	Water density of the flow [kg/m^3]
d_{50}	Mean particle diameter [m]	ρ_s	Soil particle density [kg/m^3]
d_s	Maximum scour depth [m]	μ	Dynamic viscosity of water [kg/m·s]
g	Gravitational acceleration [m/s^2]	γ_b	Bulk unit weight [gm/cm^3]
h_{si}	Maximum silting height [m]	C_u	Uniformity coefficient
L_b	Bridge length [m]	σ_g	Geometric standard deviation of the grain size distribution
L_f	Floor length [m]		
L_s	Maximum scour length [m]	F_r	Froude number
L_{si}	Maximum silting length [m]	S_o	Flume bed slope
Q	Water discharge through the flume [L/s]		
V	The mean flow velocity [m/s]		
W	Static load over the bridge [kg]		

temperature and earthquakes. The loads considered in configuration are the parts of vertical and horizontal loads. The vertical loads are opposed by the buoyancy, while the transverse and longitudinal loads are opposed by an arrangement of mooring lines or structural elements. The straight floating bridge requires securing lines or ties to guarantee adequate horizontal firmness to withstand the level stacking from wind, waves and current [9].

Compared to the conventional bridges, restricted data are accessible for floating bridges in numerous zones, (e.g. previous meteorological records and durability). As of late, it has been conceivable to design floating bridges in progressively logical and handy path due to the advancement of numerical investigation in addition the hypothetical improvements in hydrodynamic interactions among fluid and floating objects. The majority of the analytical and experimental work related to bridge dynamics expressed that there are three choices to acquire the bridge dynamic reaction which are, applying codes of practice, dynamic examination and full scale dynamic tests [10]. Most investigations are concerned with floating bridges examine them from a mechanical perspective. For instance, Wu and Sheu [11] consider the coupled heave and pitch movements of a simplified non-uniform ship body floating on a steady water surface and expose to a moving load. The impact of water depth on floating bridges conveying moving loads is contemplated by Zhang et al., [12].

Humar and Kashif [13] consider the dynamic reaction of a basically reinforced clear span bridge traversed by moving vehicles. Kristina [14] exhibit analytical models of floating bridges under moving loads and concentrated dynamic reactions with hydrodynamic impact coefficients for various depths of water. Ravi et al., [15] reveal that there are two fundamental ways to deal with be considered for floating structure; frequency and time domains. Seif and Inoue [16] contemplate the investigation of pontoon floating bridges oppressed fundamentally to wave loading with differing parameters. Parametric examinations are directed to analyze the girder response for different support structures and collision scenarios [17].

The investigation of bed morphological changes by the presence of floating bridge is required, particularly when the facilities are near the banks of flows and zones of water impact. The bed erosion is effectively produced by the crash of water waves with the structures and riverbeds. Due to the energy conveyed by water waves, the soil and rocks disintegrate from earth surface in a specific zone and move to another [18]. Contraction scour is a kind of scour that can happen if a bridge is situated in the channel width, making a tightening through the bridge foundations, foundations [19].

Numerous investigations are involved in creating and applying PC codes to reenact and foresee the contraction scour, e.g. Yong and Blair [20] demonstrate that the 2D model is satisfactory for foreseeing the contraction scour. Bui and Wolfgang [21] utilize a finite volume created model to compute the flow and dregs sediment a laboratory channel with constriction and movable bed. Luigia et al., [22] build up an approach for assessing contraction scour in clear water and unsteady flow conditions. Rajkumar [23] introduce a paper accentuates on the use of soft processing tools, for example, artificial neural network (ANN) and genetic algorithm (GA) in the expectation of scour depth with in channel contractions.

Emphasizing on studies that use experimental models concentrated on the characteristics of contraction scour; Edward et al., [24] consider the scour presented by pressure flow underneath a bridge without the limit impacts of piers or abutments. A relationship is created between pressure-flow scour and the flow conditions utilizing the exploratory information. Seungho and Irfan [25] display a physical focuses on the hydraulics of contraction scour; in light of the discoveries, a strategy for hydraulic modeling demonstrating with scaled field geometry is recommended. Hahn and Lyn [26] researched clear-water scour because of a short vertical (pressure flow) contraction in a laboratory channel. The area of maximum scour is seen to occur downstream of the contraction.

To the information of the authors, there are not many investigations that have floating bridges from a morphological perspective. Consequently, the primary targets of this paper are to examine experimentally the impact of floating bridge on the bed topography including the contraction scour under different scenarios of operations.

2. Dimensional analysis

The local bed configurations that affect the bed morphology measured in this research are as follows, [19]:

$$\phi(B, L_b, y_t, L_f, W, V, d, d_{50}, d_s, L_s, h_{si}, L_{si}, g, Q, \rho_s, \rho, \mu, S_o) \quad (1)$$

where: B = flume width, L_b = bridge length, y_t = tailgate water depth, L_f = floor length, W = static load over the bridge, V = the mean flow velocity upstream the bridge, d = bridge draft depth, d_{50} = mean particle diameter, d_s = maximum scour depth, L_s = maximum scour length, h_{si} = maximum silting height, L_{si} = maximum silting length, g = gravitational acceleration, Q = water discharge, ρ_s = soil particle density, ρ = water density of the flow, μ = dynamic viscosity of the water, S_o = flume bed slope.

The parameters can be gathered as follows: the flow characteristics (y_t, V, g, Q, μ, ρ, S_o); the bed sediment characteristics (d_{50}, ρ_s); the floating bridge geometry (B, d, L_b, W); and the bed morphological parameters (d_s, L_s, h_{si}, L_{si}).

Where in this study the impact of the viscosity is of auxiliary significance in assessing the scour parameters, and along these

lines μ is neglected, and $\frac{V}{\sqrt{gy}}$ = upstream Froude number calculated at the section where y is measured, and, B, d_{50}, L_f, S_o, and ρ are kept constant; The dimensionless products and their relationships can be written as

$$f\left(\frac{d_s}{y_t}, \frac{L_b}{y_t}, \frac{l_s}{y_t}, \frac{h_{si}}{y_t}, \frac{l_{si}}{y_t}, \frac{d_{50}}{y_t}, \frac{d}{y_t}, F_r\right) = 0 \qquad (2)$$

$$\frac{d_s}{y_t} \& \frac{l_s}{y_t} = f\left(\frac{L_b}{y_t}, \frac{d_{50}}{y_t}, \frac{d}{y_t}, F_r\right) \qquad (3)$$

3. Experimental study

The point of the experimental work is to investigate the bed morphology underneath a floating bridge giving a full portrayal for the geometry of the contraction scour and silting. The experiments are completed in Block Al-Ghannam plant, Salah al-Din Governorate, Iraq.

3.1. Experimental setup

The flume is a recycling type. It is a closed operating framework with 18 m overall length, and 0.7 m wide. The flume depth is 0.5 m at the first 10 m of its length, at that point for the following 4 m the depth is expanded by 0.25 m to be 0.75 m, at long last the depth is turned again 0.5 m at the last 4 m. It should be signified that, the 0.25 m increment in the flume depth is filled and leveled with the bed materials used in tests (Fig. 1).

The flume consists fundamentally of a head tank, glassed channel, tail tank, ground tank, and sidestep channel. Water is provided to the flume through the head tank by methods for a 3 centrifugal pumps with greatest discharge limit of 200L/s that is fitted on the ground tank. The scopes of the utilized parameters exhibit in Table 1.

3.2. Justifications of parameters assumptions

The present examination has some parameter assumptions as an essential assessment concentrated on bridge material and dimensions, static load over the bridge, discharge, and tailgate water depth. After a few of fundamental preliminary works, the parameters are:

- The bridge width is 69.5 cm (i.e. 0.5 cm less than the flume width) to allow side clearance for bridge fixation.

- The bridge height is chosen to be constant of 20 cm for practical reasons; as the used Styrofoam has 10 cm standard height and it is challenging to stick more than two pieces together.
- The bridge lengths are ranged from 50 to 70 cm; as lengths under 50 cm has greater draft explicitly in case of high loads, consequently the contraction scour increases and the total depth of bed material is completely eroded. Then again, lengths higher than 70 cm don't present detectable effect on the bed morphology particularly for experiments of low discharges and high tailgate water depth, (Fig. 2).
- The static loads over the bridge are ranged from 20 to 30 kg; as loads under 20 kg doesn't present an adequate draft to create progressive contraction scour in case of 70 cm bridge length. On the contrary, loads more than 30 kg loaded over 50 cm bridge length, the draft may be higher than the tailwater depth in a set of experiments; Fig. 2.
- The discharges are run from 50 to 110L/s; as the discharges less than 50L/s don't present an undeniable development of bed material in case of bridge of short draft, (i.e. 70 cm length and 20 kg load above). Dissimilar the discharges in excess of 110L/s lead to complete movement of the bed material explicitly for bridges of long draft, (i.e. 50 cm length and 30 kg load above).
- The tailwater depths are ranged from 12 to 16 cm; as the minimum water depth should be higher than the maximum tested draft to permit an adequate water height underneath the bridge to pass the flow. Then again, the water depths higher than 16 cm don't influence the bed topography particularly in case of low discharge tested with bridge of short draft.

3.3. Experimental procedure

After the flume is loaded up with 0.25 m depth of bed material fitted in its place in the flume, and precisely leveled (the leveling accuracy is checked by a point gauge with a precision of ±0.1 mm and leveling device). Many steps are done for each run; firstly the tailgate is totally shut, at that point the control valve at the feeding inlet is steadily opened notwithstanding back water feeding until the desired downstream water depth is approximately achieved. The pump is turned off, and the selected bridge model is introduced and deliberately fixed in its place, at that point the loads over the bridge are set and symmetrically arranged. The control valve at the feeding opening is slowly opened till keep up the required discharge, where the accurate water discharge is estimated utilizing an ultrasonic flow-meter with ±1% accuracy. The tailgate is screwed steadily until the

1- Pump   4- Sharp crest weir
2- Inlet pipe   5- Bed material
3- Stone box   6- Tail Gate

Sec (A-A)
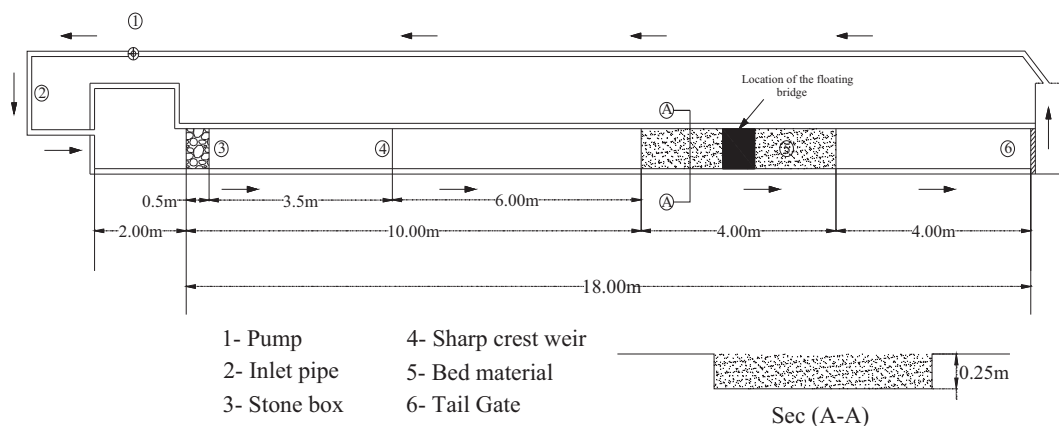
Fig. 1. The plan view of the proposed experiment.

Table 1
Range of variables used in the experiments.

Parameter	Symbol	Value	Range		Units
			From	To	
Discharge	Q	50, 70, 110	50	110	L/s
Tailgate water depth	y_t	12, 14, 16	12	16	cm
Bridge length	L_b	50, 60, 70	50	70	cm
Static load over the bridge	W	20, 25, 30	20	30	Kg
Bridge draft depth	d	4, 6, 7, 8, 9, 10.5	4	10.5	cm
Bed material	d_{50}	0.25, 0.48	0.25	0.48	mm
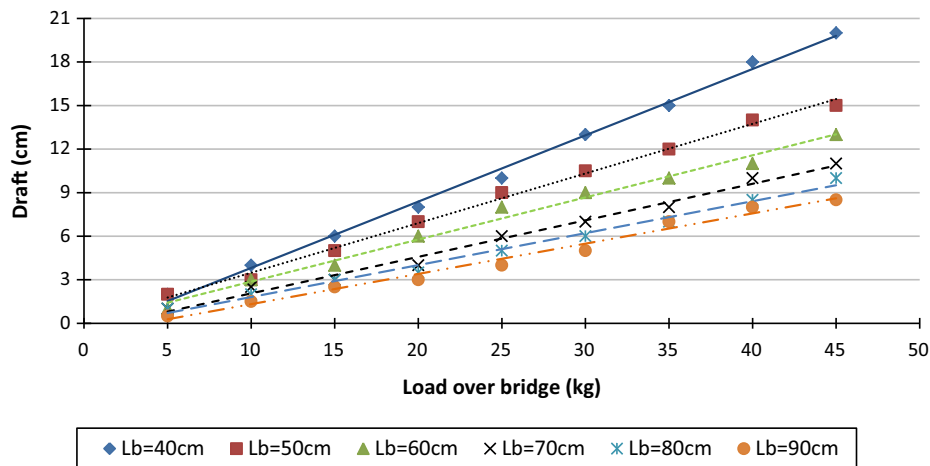
Fig. 2. The relation between load and the corresponding draft.

required downstream water depth is reached and checked utilizing the point gauge.

As of now, the running time of the test is begun, and after 4 h (where there is no appreciable changes in bed profile), the pump is turned off. The flume is discharged from water by tailgate gradually not to disturb the produced bed configuration. After the model is completely drained, the bed levels are recorded utilizing the point gauge and standard scale through the fixed grid. The previous stages are totally rehashed for each run.

3.4. Difficulties, challenges, and proposed solutions

The current experimental work has discovered some difficulties and challenges starting from test setup and wraps up by estimations. Following there are some of these difficulties and proposed solutions:

- Flume selection: the used flume is purposely looked over the point of view of dimensions, pump capacity, and feeding systems to cover the proposed scenarios.
- Uniform flow: to create a uniform flow, a screen stone box is loaded up with large gravel that implemented at the flume entrance to pass the water through to disperse flow and smothing any exorbitant turbulence, Fig. 3.
- The bridge material: The bridge material is selected to provide 3 conditions; 1- the ability of floating on the running water; 2- has adequate strength to support loads over; 3- finally, doesn't permit any volumetric change because of water absorption. Hence; the bridge material is made of Styrofoam, Fig. 4.
- Fitting the bridge: the bridge model is fitted in its place and fixed by using a fixation system consists of silicon layer to fill the small spaces between the bridge and the flume side walls and to underscore that no water spillage across these areas.

Fig. 3. The gravel box.

Fig. 4. The bridge material.

- Bridge models: to limit the costs of the Styrofoam; the tests of 70 cm bridge length are initially done and finished. A 10 cm is cutout from the bridge length to create the model of 60 cm length. Then again, the previous step is repeated for the 50 cm model.
- Load over the bridge: to guarantee an equal depth for the bridge draft, the loads are equally installed and masterminded all through 5 points; the corners of bridge model notwithstanding its middle.
- Flume filling: to avoid bed development before the run begins because of upstream water feeding, back water feeding is initially started up as well at the same time to the desired downstream water depth.
- Bed profile: the bed profile measurements are assisted through 65 points, Fig. 5 to guarantee that all bed configurations are accurately displayed. For more accuracy, the measurements are taken twice times utilizing 2 differing point gauges, and the mean values are represented.
- Bed leveling: before starting another run, the bed material is re-levelled using a sharp long stick and checked by means of leveling devices.

3.5. The scale effect

Focusing on the exploratory scale impacts, there are a few parameters are not considered in the current study because of their minor impacts which are as taking after:

The environmental parameters displayed in terms of wind and wind-induced wave motion on the floating bridge, (i.e. the dynamic response of wind that creates surface waves and current loads); The fluctuating turbulent winds and their impacts on the Aero-dynamic stability of long-span bridges; The friction of flume side walls and the viscous drag force on the bottom base of bridge model; The variations of water depth at the end of bridge model; The effect of weathering action particularly in case of of heavy rains; The seismic ground motion; At last the storm surge.

4. Model runs

The test program comprises of 168 exploratory runs using, 3 discharges, 3 tail water depths, 3 bridge models, and 3 bridge drafts by the action of 3 static loads over the bridge; Table 1. The scenarios are done to examine the impact of the previous factors on the bed topography bookkeeping the geometry of scour and deposition, Fig. 5. A planned mesh consists of 65 measuring points orchestrate in 5 lines, and 13 segment which spreads the 4 m length of bed material, Fig. 6.

To run a regression analysis model for generation numerical conditions that applied to investigate the morphological effect of the previous variables; 2 diverse bed materials are utilized. The bed materials has 0.25 m depth 4.0 m length filling the flume width are independently used. Sieve size distribution tests are done to characterize the material properties and the outcomes are laid out in table 2.

5. Results and discussions

Underlining the findings and investigation of the previous studies it's seen that Helal et al., [19] present the guidelines for current research. The novelties and motivations in this investigation come regarding the floating bridge model, the characteristics of bed material, and the flow conditions. The bridge model used in [19] is made of 4 symmetrical wooden bars with bottom intermediate spacing in the perpendicular direction of flow, one type of bed material is used which has $d_{50} = 0.62$ mm, and the range of flow condition is $0.14 \leq F_r \leq 0.25$. Regarding the current research, a solid piece of Styrofoam with level top and bottom bases is used as floating bridge model. Underscoring the bed material, 2 unique sizes of d_{50} are used, both are finer than the d_{50} used in [19]; to simulate the installation of floating bridge in waterways with soft beds. Finally, the current investigation covers more extensive scope of flow conditions than the introduced in [19] $0.105 \leq F_r \leq 0.931$.

5.1. Influence of bed material

To show bed morphological changes by the presence of the floating bridge for both bed materials handled in this study; Fig. 7 is introduced. The figure is plotted under fixed discharge, tailwater depth, bridge length, and bridge draft of 110 L/s, 12 cm, 50 cm, and 10.5 cm, respectively. The bridge draft presented by 30 kg static load. The bridge is placed somewhere in the range of 1.75 m and 2.25 m measured from the beginning of bed material as a datum, where the bridge center coincide with the center of bed material location.

It is seen that, in any case the bed material, there is no considerable movement for bed particles at the first 1 m of the bed material; where the installation of the floating bridge doesn't present in influence. At that point the contraction scouring activity begins to be actuated just upstream the bridge due to the sudden change in the current velocity based on the decrease of water depth by the action of bridge draft. However, the geometry of the contraction scour under the bridge displays in terms of depth and length is actively influenced by the bed material, but the location of the maximum scour depth continued as before that situated at 1.75 m from the bed material (i.e. upstream the bridge).

Focusing on the geometry of scour, the bed material No.1 ($d_{50} = 0.48$ mm) shows deeper scour depth and shorter scour length contrasted with bed material No.2 ($d_{50} = 0.25$ mm). That is because of the development of live bed conditions that energizes and quickens the particles development whether by rolling or transportation for bed material No.1. Additionally, that represents the development of sedimentation region just by the end of the scour hole. Concentrating on bed material No.2 of the finer d_{50},
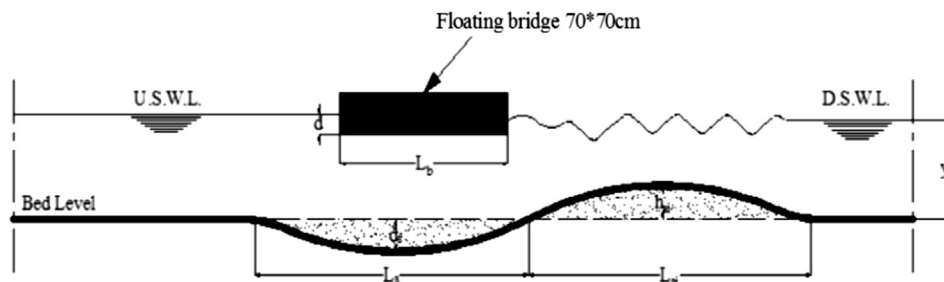
Fig. 5. Schematic diagram showing the geometry of the scour and silting, Helal et al. [19].
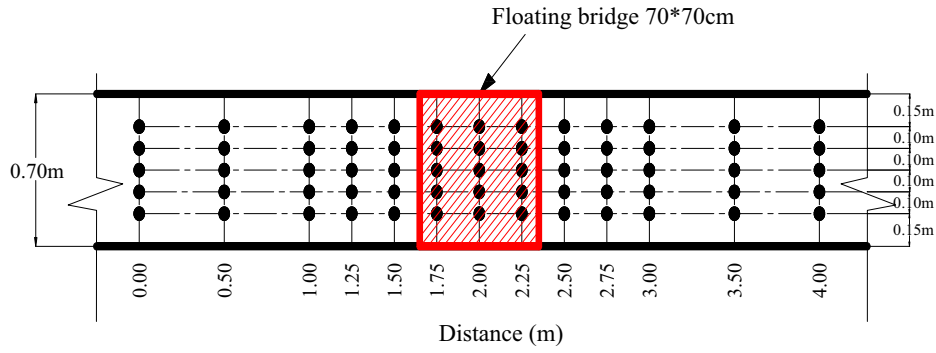
Fig. 6. Locations of bed profile measuring points.

Table 2
Characteristics of bed materials.

Bed material No.	d_{10} (mm)	d_{16} (mm)	d_{50} (mm)	d_{60} (mm)	d_{84} (mm)	γ_b (gm/cm^3)	C_u	σ_g
1	0.17	0.22	0.48	0.55	0.85	1.54	3.24	1.77
2	0.09	0.11	0.25	0.32	0.65	1.96	3.55	2.60
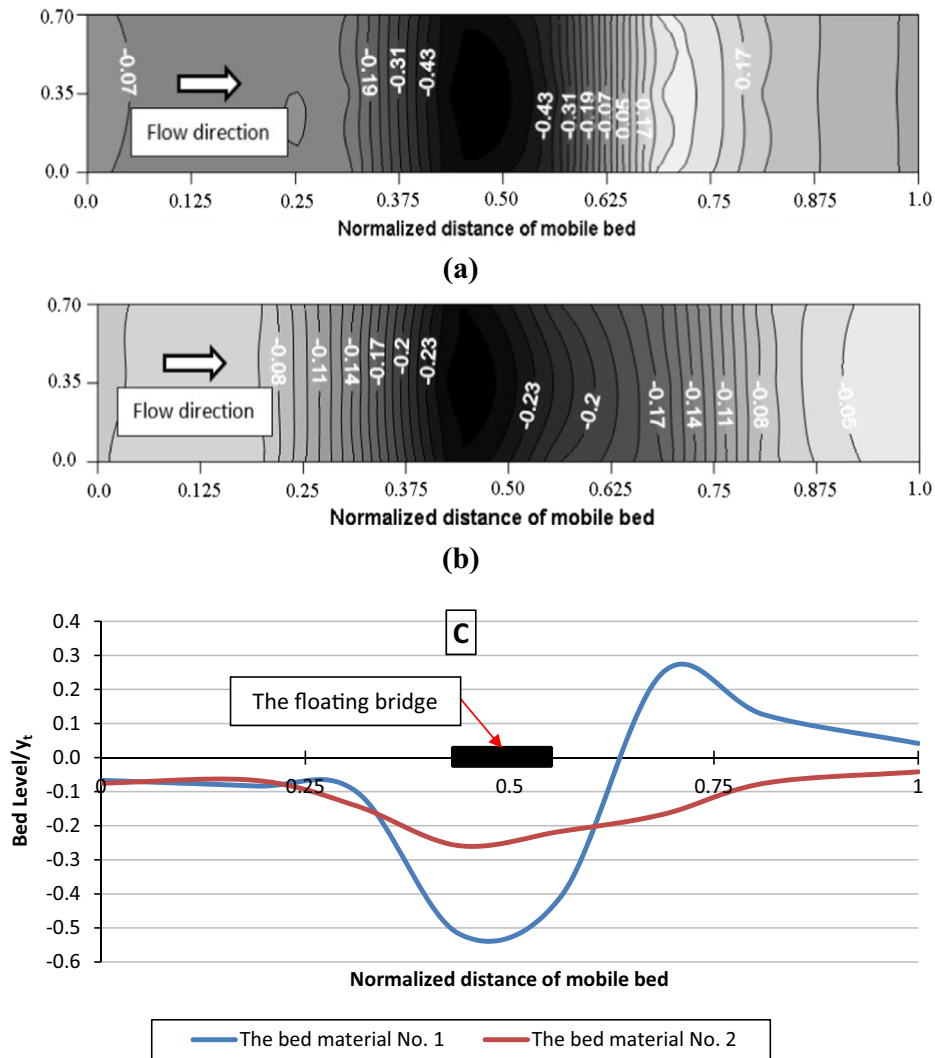
Fig. 7. Influence of bed material: (a) contour map of the scour shape for bed material No.1; (b) contour map of the scour shape for bed material No.2; (c) scour profiles in the longitudinal direction for bed materials No.1 and 2.

an armored sub-layer is achieved on the channel bed due to the particles non-consistency where σ_g = 2.6 which is considered relatively high. Thus, the erosive activity on scour depth is restricted compared to the scour length. Also, no progressive sedimentation is grown downstream the bridge which is obviously introduced in Fig. 7.

Featuring the bed length to be protected due to installation of the floating bridge, it's assessed on account the created scour length notwithstanding the scour depth. The protected bed length is started by the initiation of the scour hole upstream the floating bridge and ends once the bed level is stabilized at the downstream. Therefore, the protected length consumes the total length of the scour hole. Consequently, it's expected to find the protected length in case of bed material No.2 is longer than No.1 for comparative flow conditions and scenarios of operations.

5.2. Influence of discharge

Fig. 8 discusses the impact of discharge on the bed topographical changes related to introducing a floating bridge. The figure is plotted under fixed 50 cm bridge length, 10.5 cm bridge draft (i.e.30 kg static load over the bridge), and 12 cm tailwater depth. Regardless the bed material, it is seen that the maximum and minimum scour depths are recorded for discharges 110 and 50L/s, separately. Because of for constant tailwater depth, as the discharge increases the current velocity increases, accordingly the scouring

action is efficiently activated. Due to the short span of the used bridge model, the region of contraction scour is limited and the length of scour hole is irrelevantly impacted by the discharge. That presents a significant advantage with respect to the protection length; as there is no need to be stretched with the increase of the discharge.

Concentrating on bed material No.1, the figure shows that by the end of scour hole a district of silting is created which begins at 2.5 m and extends to 4 m. The silting locale is set up because of the large particles diameter of bed material No.1; thusly heavier possess loads which in turn hinder the particles movement to larger distances. Underscoring the geometry of silting zone, it proclaims that the silting height is straightforwardly relative to the discharge. Also, the maximum and minimum silting heights are recorded for 110 and 50L/s, individually. Exactly as the performance of the scour action; where the same quantity of particles eroded from bed are further start to deposit by the end of scour hole length.

Underscoring the bed material No.2, the figure shows that no silting zone is seen where the scour occurs for the whole length of bed material which is in actuality the bed material No.1. Likewise, the impact of discharge vanishes just downstream the bridge model owing to the end of contraction scour and the existence of the armored sub-layer.

Consolidating the discoveries of bed profiles for materials 1 and 2 it is seen that in the event that bed material No.2 the most
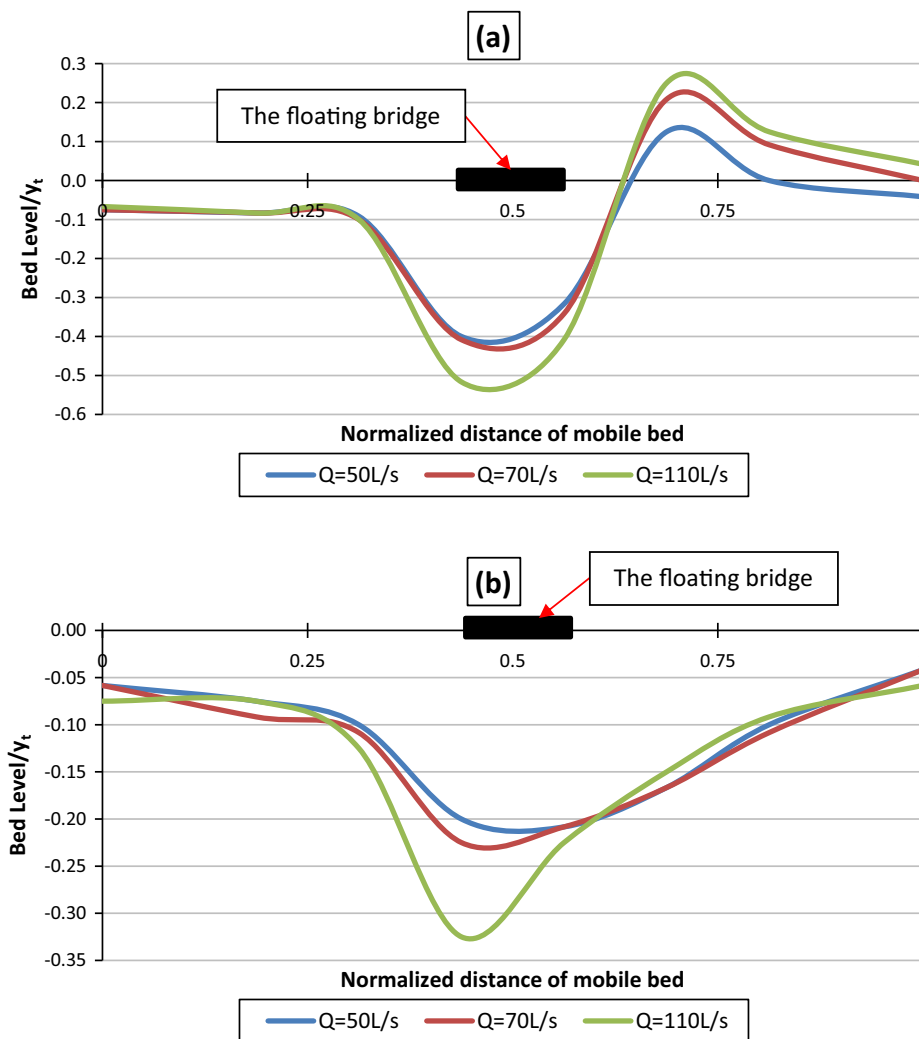
Fig. 8. Influence of discharge on: (a) bed material No.1; (b) bed material No.2.

extreme and least scour depths are decreased by 29.04% and 50.98%, separately contrasted with bed material No.1. The previous findings are accounted for the most critical scenario of operation as the discharge and the static load over the bridge. Consequently, the bridge draft are maximum while the bridge length and tailwater depth are minimum. Now, it demonstrates that the bed configurations are remarkable as the discharge increase.

5.3. Influence of bridge draft

In a comparison of static and dynamic experiments, it is seen that the dynamic investigations give roughly indistinguishable patterns from the static analyses with respect the geometry of the contraction scour [19]. Thusly in the present study, the static investigations are only concluded. Where the bridge draft results by the presence of the static load over the floating bridge; Fig. 9 presents impact of the bridge draft on bed. The figure is plotted under fixed 110L/s discharge, 50 cm bridge length, and 12 cm tailwater depth; where the most extreme turbulences in bed profile are expected to occur for various bridge drafts. The figure demonstrates that the maximum and minimum scour depths are recorded by 10.5 and 7 cm bridge drafts, individually for the two bed materials. The bridge drafts are corresponding to static load over the bridge of 30 and 20 kg, respectively. Consequently, it is reasoned that the geometry of scour and sedimentation is legitimately corresponding to the bridge draft. These discoveries can

be clarified that as the static load increment the bridge draft increments as well; Fig. 2. Thus, the water depth diminishes underneath the bridge accordingly the velocity and thus the contraction scour. A similar bed profile pattern in Fig. 8 is rehashed in Fig. 9; where at the first 1 m the bed topography is unconcerned by the tested variable notwithstanding the particles diameters. Concentrating on bed material No.1 the figure presents that a sedimentation zone is formed downstream the bridge and its height is observed increases as the static load over the bridge and the bridge draft increase. Focusing on the scour hole tended to by bed material No.2 it pronounces that the maximum and minimum scour depths are decreased by 35% and 73.31% individually contrasted with bed material No.1 for the most critical run in view of similar reasons discussed in Section 5.2. Therefore, it is concluded that the bed topographical changes are legitimately relative to the bridge draft and accordingly the static load.

5.4. Influence of bridge length

Fig. 10 demonstrates the impact of bridge length on bed. The figure is plotted under fixed 110 L/s discharge, 10.5 cm bridge draft (i.e. 30 kg static load over the bridge), and 12 cm tail water depth which are considered the critical variables that create the maximum turbulence underneath the floating bridge model for the 3 tested lengths. The figure demonstrates that for both bed materials, the greatest and least scour depths are found in case of bridge
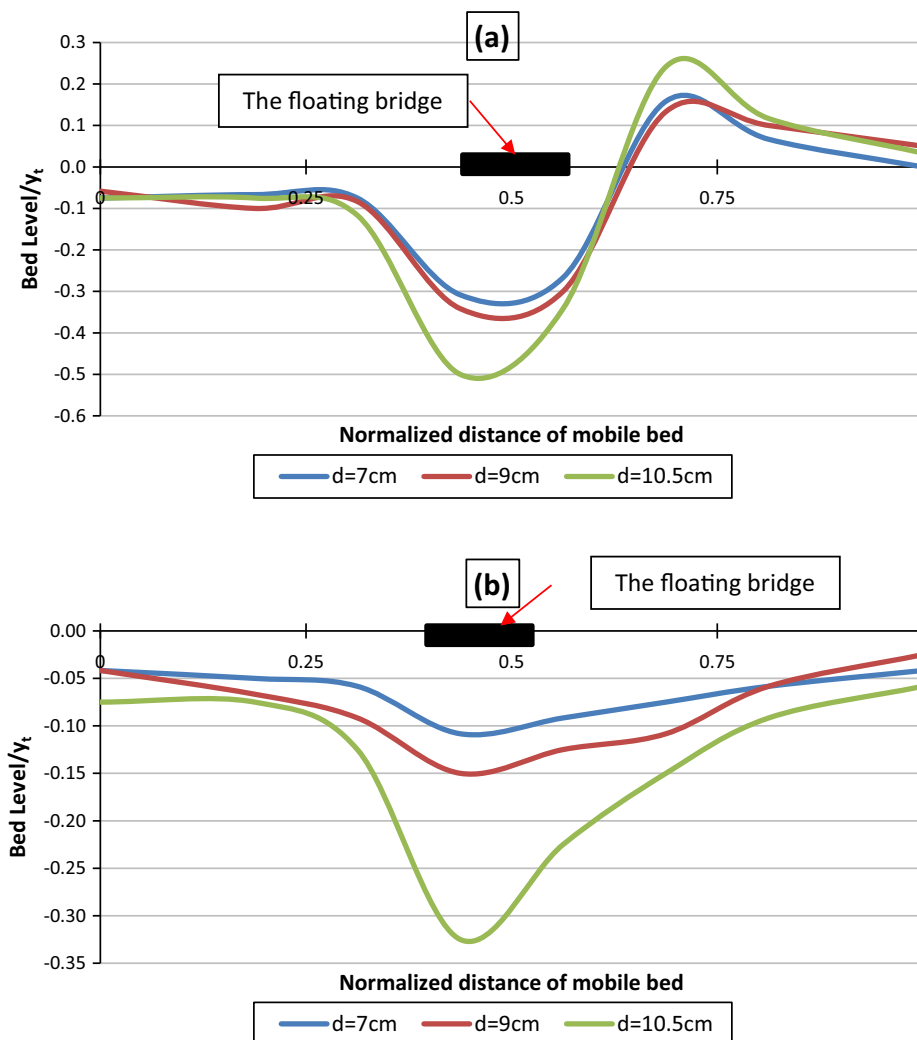
Fig. 9. Influence of bridge draft on: (a) bed material No.1; (b) bed material No.2.
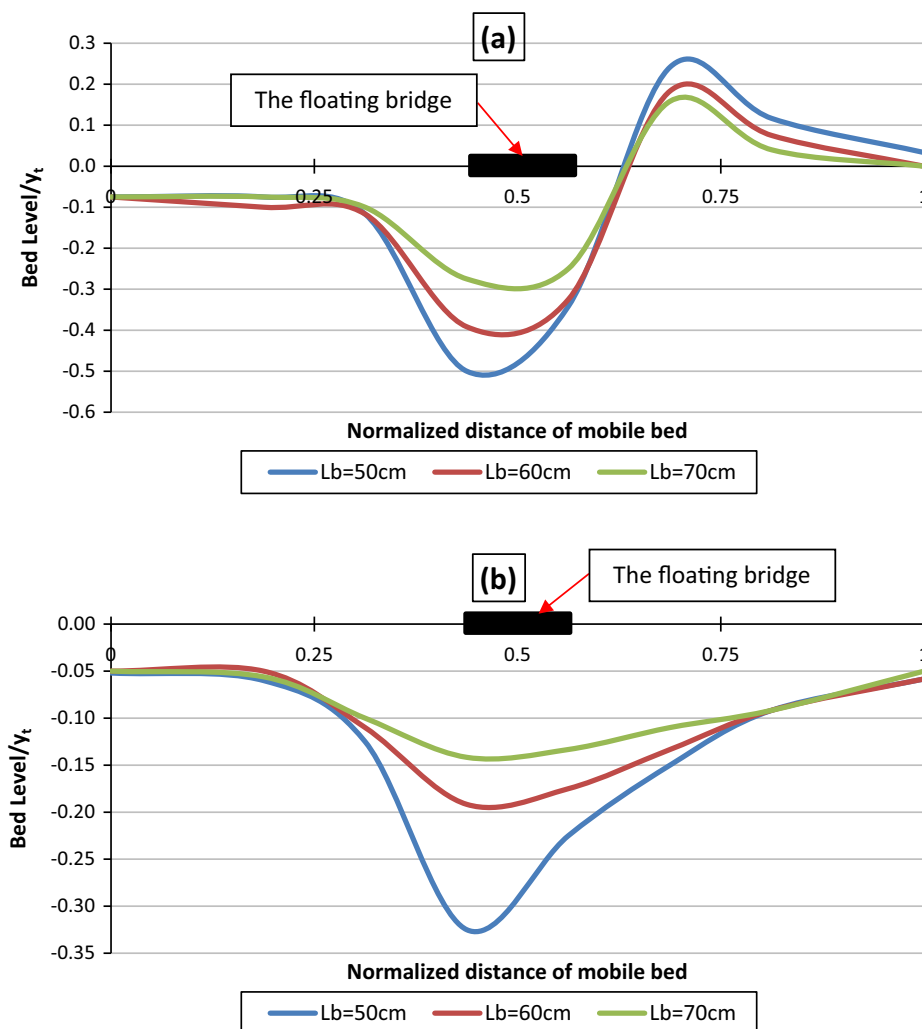
Fig. 10. Influence of bridge length on: (a) bed material No.1; (b) bed material No.2.

lengths of 50 and 70 cm, separately where the bridge drafts are 10.5 and 7 cm, respectively, Fig. 2.

That can be outlined that for constant static load over the bridge, as the bridge length increment the contacted area exposes to higher upward buoyant force. Subsequently, the draft decrease then the contraction scour as well. A similar pattern is obviously seen for each bed material where the area of maximum scour stays unaltered simply upstream the bridge. Likewise, an area of sedimentation is created in case of bed material No.1.

From figure investigations that presented for the critical condition it is seen that increasing the bridge length 10 cm (from 50 to 60 cm) prompts 27.87% and 41.23% decrease maximum scour depth for bed material No.1 and 2, individually. However, increasing the bridge length 20 cm from (50–70 cm) prompts 45.01% and 56.61% decrease in maximum scour depth for bed material No.1 and 2, individually. Concentrating on the area of sedimentation it is discovered that the silting height diminishes by 24.06% and 34.44% for 60 and 70 cm bridge lengths contrasted with 50 cm bridge length. Thus, it very well may presume that the bed morphological changes are conversely relative to the bridge length.

5.5. Influence of tailwater depth

Fig. 11 shows the impact of tailwater depth on bed. The figure is plotted for the most critical flow condition regarding the maximum discharge, bridge draft, and minimum bridge length. The tests are carried out under fixed 110L/s discharge, 50 cm bridge length, and 10.5 cm bridge draft (i.e.30 kg static load over the bridge).

The figure exhibits that the greatest and least scour depths are found at 12 and 16 cm tailwater depth. Likewise, accentuating the area of sedimentation that figured in case of bed material No.1 it is seen that the most extreme and least silting heights are situated at 12 and 16 cm tailwater depth. Along these lines, it tends to be presumed that the unsettling influence in bed profile by the presence of floating bridge is contrarily corresponding to the tailgate water depth notwithstanding the type of bed material. That can outlined for constant discharge and bridge draft, as the tailwater depth decrease the current velocity increase and contraction scour acts effectively.

Moreover, unnoticeable impact of tailwater depth on the scour length is displayed. Concentrating on the scour depth, because of the fine particle size of bed material No.2, it is less sensitive to the fluctuations of tailwater depths compared to bed material No.1 of larger particle size.

Regarding the most critical scenario where the maximum flow turbulences are found, on account of bed material No.1, the scour depth is increased by 13.04% and 30.43% for 14 and 16 cm contrasted with 12 cm tailwater depths. Then again the instance of bed material No.2, the scour depth is increased by 32.01% and 56.03% for 14 and 16 cm contrasted with 12 cm tailwater depths. Therefore, it remarks that the bed morphological changes are inversely to the tailwater depth.
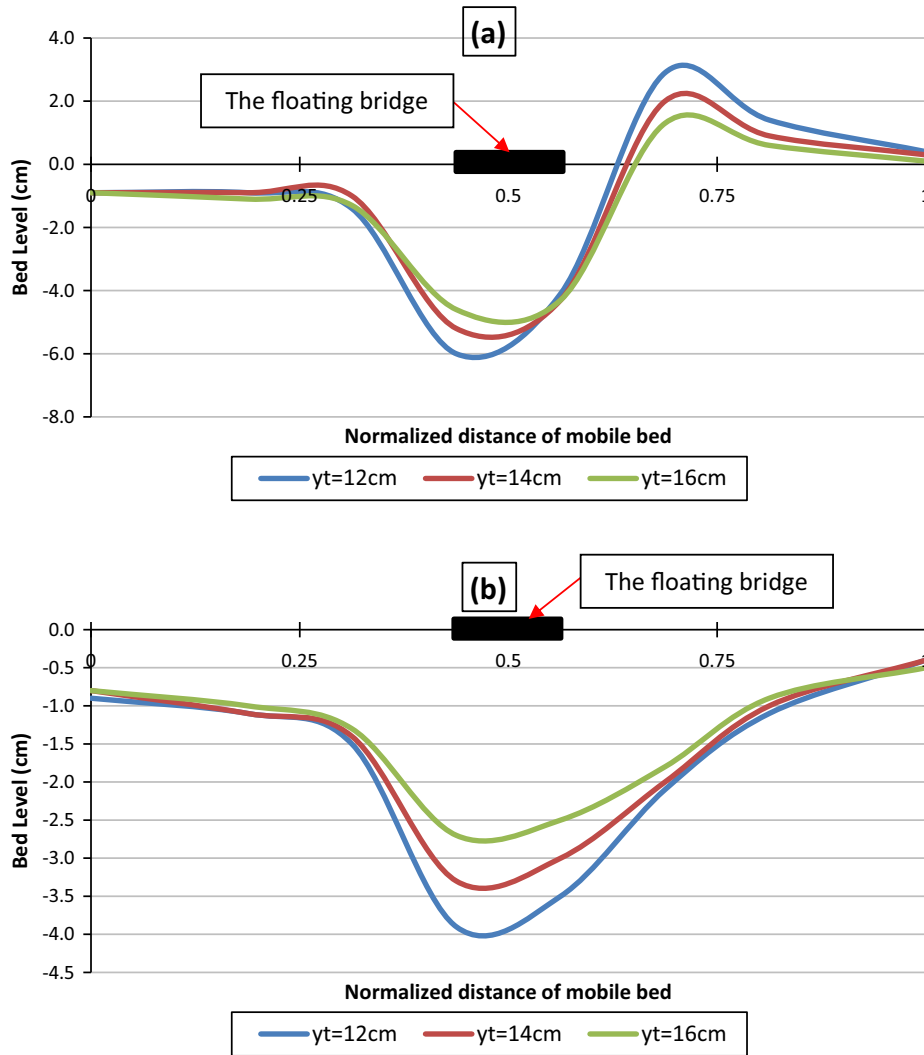
Fig. 11. Influence of tailgate water depth on: (a) bed material No.1; (b) bed material No.2.

The experimental outcomes are utilized for relating the diverse dimensionless variables for developing empirical formulae to register the characteristics of the contraction scour introduced in terms of depth and length. With the assistance of nonlinear regression investigation, the accompanying experimental recipes are inferred:

$$\frac{d_s}{y_t} = \exp\left[-0.136\left(\frac{L_b}{y_t}\right) + 381.86\left(\frac{d_{50}}{y_t}\right) + 1.06\left(\frac{d}{y_t}\right) + 0.238F_r - 2.82\right] \tag{4}$$

$$\frac{L_s}{y_t} = \exp\left[0.078\left(\frac{L_b}{y_t}\right) - 133.71\left(\frac{d_{50}}{y_t}\right) + 0.69\left(\frac{d}{y_t}\right) + 0.027F_r + 2.01\right] \tag{5}$$

The coefficients of determination (R^2) for Eqs. (4) and (5) are 0.887 and 0.801, respectively. Eqs. (4) and (5) are valid for the following conditions: $50 \leq Q \leq 110$L/s; $0.105 \leq F_r \leq 0.931$; $3.125 \leq \frac{L_b}{y_t} \leq 5.833$; $0.0015 \leq \frac{d_{50}}{y_t} \leq 0.004$; $0.25 \leq \frac{d}{y_t} \leq 2.5$.

From Eqs. (4) and (5) it tends to be presumed that the particles size of bed material is the main factor that influences the scour depth and length; where increasing the d_{50} increase the scour depth, and lessening the scour length. It is likewise seen that $\frac{d}{y_t}$ has the following most prominent impact on the scour parameters. For the flow conditions utilized, it is seen that reducing the values of F_r decrease the scour parameters. At last, as the bridge length increment the scour depth diminishes and the scour length expands.

To check the adequacy of the derived equations; Fig. 12 is plotted to exhibit the relation between the measured scour depth and length contrasted with the calculated values utilizing Eqs. (4) and (5). Regarding the scour depth, Fig. 12 demonstrates that the calculated values coordinated with the measured with most extreme ± 8% of error. However the percentage of errors is increased to ± 10% for the scour length. That agreed with the derived coefficients of determination for Eqs. (4) and (5).

6. Conclusions

The experimental study to explore the bed morphological changes resulted in the presence of floating bridge are carried out within the range of used data and prompts the accompanying conclusions:

- The discharge is the most active parameter that influences the bed topography, however the tailwater depth has the least impact.
- To shield the bed material from scouring, the channel must be lined at the site of the floating bridge. The minimum upstream protection length has to be $2y_t$ regardless the diameters of bed
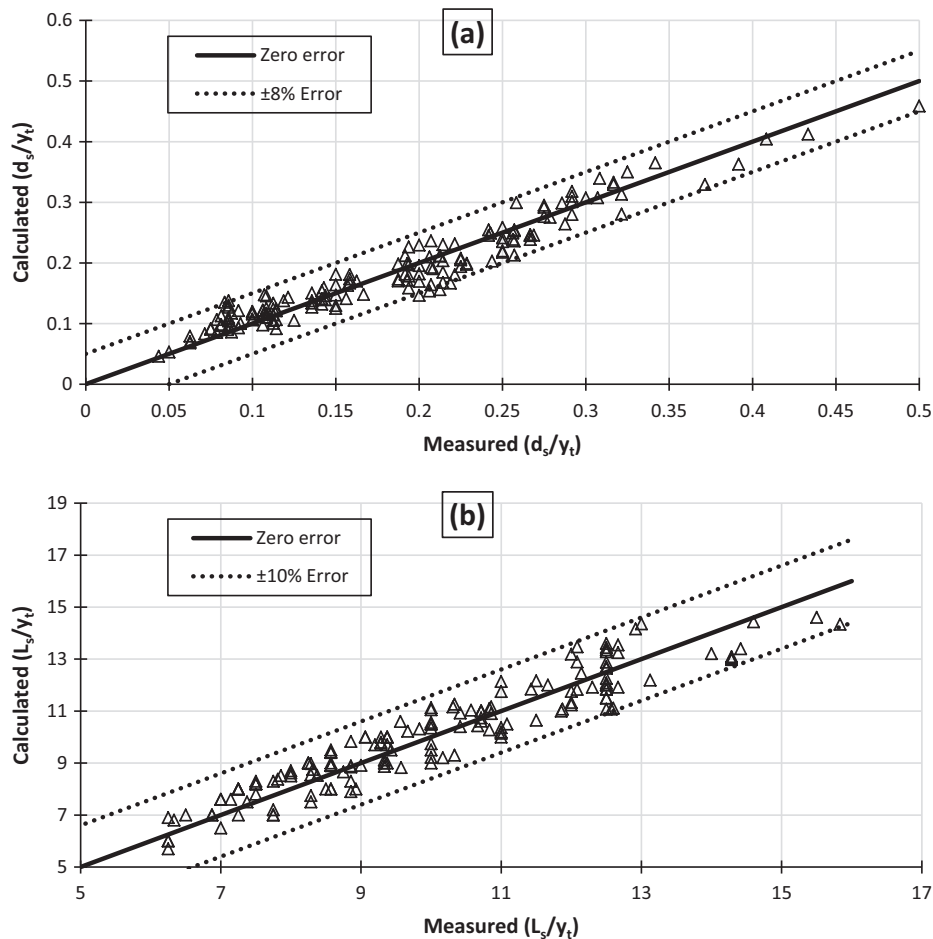
Fig. 12. Comparison between measured and calculated values for: (a) d_s/y_t; (b) L_{smax}/y_t.

material, which agreed with [19]. However, the minimum downstream protection length has to be $4y_t$ and $12y_t$ in case of bed material No.1 and 2, respectively.

- The morphological changes are imperceptibly at the first 1 m upstream the bridge as most of changes are located underneath and downstream the bridge.
- The maximum scour depth is located just upstream the bridge under any flow condition.
- The influence of any tested parameter is highlighted on the scour depth, however it can be ignored on the scour length.
- Regardless the bridge length and draft, the morphological changes increase as the discharge increment and tailwater depth decline.
- Under fixed bridge length, the bridge draft increase as static load over the bridge increase, leading to decrease the flow depth underneath the bridge, subsequently the bed morphological changes are remarkable.
- For fixed bridge draft, the morphological changes increase as the bridge length decrease.
- Under any flow condition, as the diameters of bed material decrease, the scour length increase however the scour depth decrease.

Declaration of Competing Interest

The authors declare that they have no known competing financial interests or personal relationships that could have appeared to influence the work reported in this paper.

References

[1] Daniel VJ. Numerical and Experimental Investigation of Ribbon Floating Bridges. Ottawa, Ontario: Master of Applied Science in Civil Engineering, Carleton University; 2018.
[2] Lwin MM. Floating Bridges. In: Chen Wai-Fah, Duan Lian, editors. Bridge Engineering Handbook. Boca Raton: CRC Press; 2000.
[3] Watanabe E, Utsunomiya T. Analysis and design of floating bridges. Prog Struct Mat Eng 2003;5(3):127–44.
[4] Petersen L. Siege Warfare and Military Organization in the Successor States (400–800 A.D.). Leiden: Brill Publishers; 2013.
[5] Faruque Hossain Md. Sustainable Design and Build: Building, Energy, Roads, Bridges, Water and Sewer Systems. Butterworth-Heinemann; 2018.
[6] Wang CM, Wang BT. Large Floating Structures. Technological Advances. Singapore: Springer Singapore; 2015.
[7] Zhengshun C, Zhen G, Torgeir M. Numerical Modeling and Dynamic Analysis of a Floating Bridge Subjected to Wind, Wave, and Current Loads. J. Offshore Mech. Arct. Eng 2018;141(1):1–18.
[8] Sha Yanyan, Amdahl Jørgen, Aalberg Aleksander, Zhaolong Yu. Numerical investigations of the dynamic response of a floating bridge under environmental loadings. J Ships Offshore Struct 2018;13(1):1–19.
[9] Senderud K. Modelling and Analysis of Floating Bridge Concepts Exposed to Environmental Loads and Ship Collision Master thesis. Norwegian University of Science and Technology; 2018.
[10] Paultre P, Proulx J, Talbot M. Dynamic testing procedures for highway bridges using traffic loads. J Struct Eng ASCE 1995;121(2):362–76.
[11] Wu JS, Sheu JJ. An exact solution for a simplified model of the heave and pitch motions of a ship hull due to a moving load and a comparison with some experimental results. J Sound Vib 1996;192(2):495–520.

[12] Zhang J, Miao GP, Liu JX, Sun WJ. Analytical models of floating bridges subjected by moving loads for different water depths. J Hydrodyn 2008;20 (5):537–46.

[13] Humar JL, Kashia. Dynamic response of bridges under travelling loads. Can J Civ Eng 1993;20:287–98.

[14] Kristina HL. Description and Analysis of Floating Bridges Master thesis. Norwegian University of Science and Technology; 2017.

[15] Ravi C, Pulkit S, Hemant. Review Paper on Submerged Floating Tunnels. Int J Eng Technol Sci Res 2018;5(4):345–50.

[16] Seif M, Inoue Y. Dynamic analysis of floating bridges. Mar Struct 1998;11. 1–2/2:29–46.

[17] Yanyan S, Jørgen A, Cato D, Zhaolong Yu. Numerical Investigation of the Collision Damage and Residual Strength of a Floating Bridge Girder. In: 37th International Conference on Ocean, Offshore and Arctic Engineering. p. 11A.

[18] Blaikie Piers. The Political Economy of Soil Erosion in Developing Countries. 1st ed. London: Routledge; 2016.

[19] Helal E, Sobeih Mohamed, Ezz El-din M. Effect of Floating Bridges on Open Channels' Flow and Bed Morphology. J. Irrig. Drain Eng. 2018;144(9).

[20] Lai Yong G, Greimann Blair P. Predicting Contraction Scour with a 2D Model. World Environmental and Water Resources Congress 2008 May 12–16, 2008 | Honolulu, Hawaii, United States, 2008.

[21] Duc Bui Minh, Rodi Wolfgang. Numerical Simulation of Contraction Scour in an Open Laboratory Channel. J Hydraul Eng 2008;134(4).

[22] Brandimarte Luigia, D'Odorico Paolo, Montanari Alberto. A probabilistic approach to the analysis of contraction scour. J Hydraul Res 2006(5):654–62.

[23] Raikar Rajkumar V, Wang Chuan-Yi, Shih Han-Peng, Hong Jian-Hao. Prediction of contraction scour using ANN and GA. Flow Meas Instrum 2016;50:26–34.

[24] Umbrell Edward R, Kenneth Young G, Stein Stuart M, Sterling Jones J. Clear-Water Contraction Scour under Bridges in Pressure Flow. J Hydraul Eng 1998;124(2).

[25] Hong Seungho, Abid Irfan. Physical model study of bridge contraction scour. KSCE J Civ Eng 2015;20(6):1–8.

[26] Hahn EM, Lyn DA. Anomalous Contraction Scour? Vertical-Contraction Case. J Hydraul Eng 2010;136(2).

Mohamed M. Ibrahim has M.Sc. and PhD in Water resources and Hydraulics from Benha University, Egypt. He is specialist in open channel hydraulics. He is currently works as Professor Associate at Shubra faculty of engineering, Benha University.

Mohammed A. Hassan has M.Sc. and PhD in in Water resources and Hydraulics from Benha University – Shubra College of Engineering. He is currently an Assistant Professor at Shubra faculty of engineering, Benha University.

Adnan D. Ghanam has a B.Sc. in Civil Engineering from Mosul University. He is currently Member of Iraqi council of representatives and General Director of Iraqi Cement Company in the Ministry of industry and Minerals.